Proceedings of The Canadian Society for Mechanical Engineering International Congress 2018
CSME International Congress 2018
May 27-30, 2018, Toronto, On, Canada

WIND LOADS ON CYCLISTS DUE TO PASSING VEHICLES

William David Lubitz*, Bryan Rubie
School of Engineering
University of Guelph
Guelph, Canada
*wlubitz@uoguelph.ca

Abstract— Cyclists on rural highways travel at much lower speeds than motor vehicles. There is concern that unsteady aerodynamic loads produced as a large vehicle passes a cyclist can cause instability and loss of control, potentially initiating a traumatic accident for the cyclist. Large lateral spacing can be provided between cyclists and motor vehicles using wider paved shoulders, however this adds cost to road construction, so there is a need to balance the needs of cyclist safety and paved shoulder width. Understanding the nature of the unsteady wind loads experienced by a cyclist when a motor vehicle passes is a necessary first step in determining optimum paved shoulder widths. An experiment was conducted that directly measured the lateral forces on a full scale model cyclist, static pressure and wind speed as motor vehicles passed a cyclist. As a motor vehicle passed, the cyclist first experienced a large transient lateral forcing, followed by lower magnitude forcing. The magnitude of the force was well correlated to the measured static pressure, while induced transient wind speeds were relatively low (on the order of 1 m/s). As would be expected, the magnitude of forcing increases with vehicle size and speed, and decreases as lateral spacing between cyclist and vehicle increases. The results were used to develop an expression to predict tipping moment as a function of passing vehicle characteristics and offset distance.

Keywords-bicycle; wind load; aerodynamics; passing vehicles

I. INTRODUCTION

The passing of a large vehicle like a truck can be an unsettling experience for a cyclist travelling on a rural highway. The wakes of large vehicles produce aerodynamic forces on cyclists and other road-side objects. There is concern that unsteady lateral forces on a cyclist produced by a large passing vehicle could cause a cyclist to become unstable and lose control, potentially initiating a traumatic accident.

If available, cyclists on rural highways generally utilize paved shoulders for travel, allowing them to travel outside the regular travel lane. Wider paved shoulders allow cyclists to travel with greater lateral separation from large vehicles, reducing the aerodynamic forces experienced by a cyclist induced by passing vehicles. However, shoulder paving cost increases with width, and the safety benefits of increased shoulder paving width must be balanced with costs [1]. Currently, information is still needed on minimum safe lateral spacing between the travel paths of bicycles and large vehicles on rural highways. Minimum safe spacing depends on the aerodynamic forces induced on a cyclist by large vehicles passing at highway speeds, and the maximum such forces that a cyclist can experience and remain stable [2].

There is little quantitative information available on the forces induced on cyclists by wakes generated by passing large vehicles. Several publications on bicycle infrastructure design [3-5] reproduce the same plot of lateral aerodynamic "force" exerted on a cyclist by a passing truck as a function of speed and separation distance (Fig. 1). A 1976 US government report [6] was the earliest incarnation of this plot that was found. No information on the source of the plot was provided except a note that it was from "prior research."

It is apparent Figure 1 is at best an idealization. While force is approximately proportional to the square of the vehicle velocity, the linear relationship between separation distance and force seems physically unlikely. The reporting of a force in units of mass (kg) is worrisome (note that lbs was used by Smith [6]), and it is unclear if average or peak lateral forces are reported. No guidance is given on how the estimated tolerance limit of 1.73 kg (17 N) was derived. Despite these limitations, the 17 N lateral force limit and Fig. 1 appear to be the current accepted standard in the bikeway design literature for aerodynamic forces on cyclists due to passing vehicles. For example, Llorca et al. [2] recently applied this same linear relationship with zero effect at 3.0 m in their analysis of motor vehicles passing cyclists.

Only one prior study was located that attempted to directly measure the wind loads that would be induced on a cyclist (as opposed to other object) by a passing vehicle [7]. Two propeller anemometers were placed at the roadside, and the induced wind was measured as a heavy goods truck was driven past at a range of speeds and offset distances. However, the impact on a cyclist was estimated using assumptions of cyclist area and drag coefficient, rather than by a more direct form of measurement. They observed that as the truck passed, a wind speed "pulse" occurred in the lateral direction that was first away from, and then towards, the direction of the vehicle. As vehicle speed increased, the amplitude of this pulse increased while the time duration decreased, and it was noted that the rapid change in wind direction was likely to be particularly destabilizing.

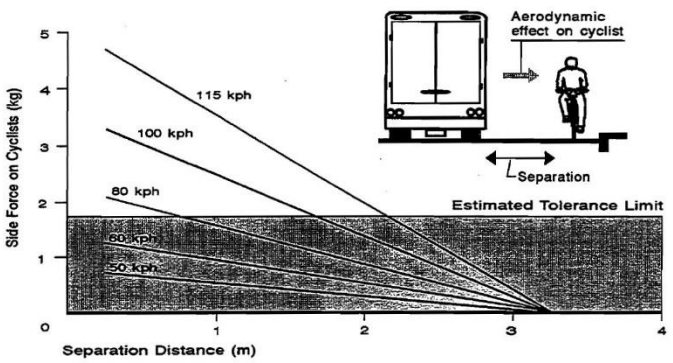

Figure 1. Aerodynamic force on a cyclist due to a passing large truck. From [4].

Research has been conducted in the similar areas of wind loads caused by large trucks on overhead sign bridges [8], temporary roadside signs and barriers [9] and pedestrians [10]. Recently, Lichtneger and Ruck [11] experimentally measured forces on a range of plates beside and above passing vehicles ranging from passenger cars to large buses and trucks (lorries). The winds induced on railway station platforms due to passing express trains have also been studied [12, 13].

While these studies encompass a range of situations and investigative methods (field measurements, simulations, theory), they agree on the features of the aerodynamic forcing experienced by a stationary or relatively slow moving object (such as a bicycle) being passed closely by a high-speed vehicle. The most concerning effect of a passing large vehicle is an initial sharp pulse of increased pressure, which occurs over a time period of a few tenths of seconds, and is followed immediately by a period of decreased pressure. This is accompanied by wind speed gusts on the order of 1 m/s, also over a time period of order 0.1 s. The magnitude of these pressures and gusts increases with frontal area of the passing vehicle and decreases with vehicle streamlining. The initial pressure pulse is followed by increased turbulence and a return to pressures nearer ambient. The passage of large gaps in vehicles (e.g. between truck cab and trailer) and the blunt tail of a vehicle also induce pulses of pressure and wind speed variation from ambient levels, although these are typically lower than those associated with the passing of the front of the vehicle. An example of the transient forcing, pressure and air speed from the experiments for this project is shown later in Fig. 4.

There are a few important differences between the case of lateral forcing on a moving cyclist that could cause loss of balance, and forcing of stationary objects such as signs and walls. First, while all prior literature has focused on forces on cyclists or other surfaces, arguably the most important phenomena from the passing of a large vehicle would be not a transient lateral force on the cyclist, but rather the resulting transient lateral moment around the contact line between the wheels and the road surface. A lateral force exerted only a centimeter above the ground would do much less to unbalance a traveling cyclist than the same force exerted at the level of the cyclists shoulders or head (provided the wheels do not slide sideways, which given the forces we will discuss below is a reasonable assumption). In the experiments and discussion that follow, it will be lateral moments that are measured and considered, rather than just lateral force, although at times "force" will be used because moment will be the force measured by a load cell multiplied by a known moment arm.

The time periods of transient forcing of the cyclist are also very important. Unlike signs or walls, cyclists actively respond to transient forcing, by adjusting steering and body position, in order to maintain a balanced riding position. A cyclist could easily respond to a large force (or moment) being applied smoothly and gradually over a long period of time. However, the same forcing applied in a few milliseconds could cause an immediate instability that would be very difficult to correct and could lead to a loss of balance. Unlike for fixed objects, forcing timing matters, as does the nature of the cyclist's response.

Bicycle-specific measurements of the aerodynamic forces induced by large passing vehicles are still needed. It is not feasible to calculate highly accurate wind and pressure forces on a bicycle and rider because they are a geometrically complex bluff-body, unlike the uniform flat plate or cylindrical tubes typical of highway signs and sign bridges, immersed in a highly transient flow. While there is a large body of research on the aerodynamics of both cyclists and motor vehicles, most has been conducted with the goal of reducing the steady state aerodynamic drag of the vehicle itself. These studies don't address crosswinds or unsteady flow, and are of little use for this research. Also, studies that do investigate crosswinds are generally not directly applicable. For example, Moulton et al. [14] investigated the crosswind loads on a streamlined bicycle, and Tew and Sayers [15] measured crosswind effects on bicycle wheels. However, different forces due to crosswind effects would be expected for a conventional upright non-streamlined bicycle (which is essentially a collection of bluff bodies), rather than a rotating wheel or streamlined human powered vehicle. The authours could find no direct measurements of lateral aerodynamic forces on a non-racing cyclist due to transient events such as passage of a large vehicle.

Given the temporal and spatial transience of the flow, this situation cannot be reliably modelled using CFD tools unless field data is available to validate the CFD simulations. The geometry of an unstreamlined bicycle and rider is quite complex, and it is not feasible to directly measure the induced pressures using pressure taps. Therefore, measuring the forces induced on a full size bicycle was selected as the most feasible approach. This research project sought to address this lack of fundamental data by directly measuring the lateral force caused by passing vehicles on upright, diamond frame, single rider, non-streamlined bicycles. It should be noted that the experiment documented below was a relatively modest, resource-constrained affair. While some conclusions are provided to some of the questions and issues raised above, significant scope remains for additional experimental study.

II. METHODOLOGY

A stationary instrumented bicycle with full scale model rider, three-dimensional sonic anemometer (RM Young 81000) and omni-directional static pressure sensor were placed in a line adjacent to the vehicle travel path in Fig. 2. The test vehicle would first pass the model cyclist, than the pressure probe, and last the sonic anemometer. Horizontal spacing was 1.20 m between the

centers of the anemometer and pressure probe, and 1.00 m between the pressure probe center and the leading edge of the front bicycle tire. The anemometer and pressure probe were mounted on vertical poles at a sampling height of 1.15 m. Lateral moment on the bicycle, static pressure and three-dimensional wind speed were measured simultaneously as vehicles passed.

Static pressure was measured using a parallel plate two-port static pressure probe like that of Robertson [16]. A Setra 265 differential pressure transducer was mounted immediately below the pressure probe. The reference side of the transducer was connected to a rigid tank housed within an insulated container (the white box in Fig. 2) that included a small rigid syringe to allow setting of the reference pressure, allowing recording of both positive and negative pressures relative to ambient pressure.

Characteristics of the truck and the model bicyclist are summarized in Table 1. Projected areas and centroids were determined by analysis of photographs taken specifically for measurement purposes using a long telephoto lens to minimize parallax errors. ImageJ (https://imagej.nih.gov/ij/) was used for the actual image analysis.

All testing was done on a closed course. Cones and pavement markings located prior to the bicycle and sensors allowed the vehicle driver to laterally position the vehicle as it passed the instruments. Two optical switches placed on the roadway 10 m apart adjacent to the instruments directly measured the speed of the passing vehicle. The distance between vehicle path and the line of instruments was measured directly by wetting the roadway before the vehicle passed, and measuring the distance to the tire tracks left by the vehicle immediately after it passed. The method was accurate to ± 1 cm.

The bicycle wheels were set in a low-profile heavy aluminum channel, and the tires were inflated to a very high pressure to produce minimal resistance to rotation in the lateral direction. The bicycle brakes were permanently set to prevent forward or backward rolling of the bicycle. A dummy rider was constructed incorporating a solid wood, metal and plastic frame, plus additional packing material inside a full length 8 mm neoprene wetsuit. Boots, a foam head and cycling helmet and diving gloves were attached rigidly to the body frame at the locations of feet, head and hands. The dummy was rigidly affixed to the bicycle at the handlebars and pedals, positioned in a semi-upright riding position. The dimensions of the combination bicycle and rider are also given in Table 1.

Lateral force on the model cyclist was directly measured using a custom-built load cell. A temperature-compensating load cell was constructed by placing four surface-mount strain gauges wired in a full Wheatstone bridge on the surface of a thin wall aluminum tube. Spherical rod-end joints were placed at each end of the tube. The tube was oriented horizontally with one end connected to the downtube of the bicycle above the pedals at a height of 0.59 m above the ground. The other end was affixed to a heavy low-profile rigid frame. The load cell provided the only lateral support of the bicycle. Before each set of tests the load cell was calibrated in-situ using precise weights and a pulley system to apply tensile and compressive lateral forces up to 15 N. The Wheatstone bridge was connected via shielded cables to a custom-built amplifier.

All instrumentation was connected to a netbook computer using a National Instruments USB-6008 data acquisition device (for switches, barometer, load cell, lateral component of wind speed) and serial-to-USB converter (all anemometer channels). A custom-written LabView application simultaneously collected and stored measurements of optical switch output, pressure, force and lateral wind speed component at 1000 Hz. Note that the update rate of the anemometer was 32 Hz, meaning that the lateral wind speed is oversampled. Additionally, all channels of anemometer output (three wind speed components and temperature) were recorded at a rate of 32 Hz by recording the anemometer serial output.

Table 1. Vehicle and model cyclist parameters.

Parameter	Model Bicyclist	Truck
Description	Semi-upright, with helmet, on 26" wheel mountain bike	2001 Dodge Ram, 4 wheel drive, full size pickup truck
Drag Coefficient	0.9 – 1.1 [17]	0.47 [18]
Frontal Area	0.74 m^2	3.17 m^2
Overall Height	1.72 m	1.84 m
Overall Length	1.67 m	5.49 m
Side Area	0.71 m^2	
Centroid Height Above Ground	0.87 m	
Centroid Horizontal Distance from Front	0.94 m	

III. RESULTS

Data was collected for passes of the truck at a range of offset distances and vehicle speeds, as shown in Fig. 3. Maximum speeds were limited by the need to bring the vehicle up to test speed, settle at that speed, pass through the test area, and decelerate safely. Pressure, wind and loading fluctuations were negligible when the truck passed at a speed of U_v less than 30 km/h.

Figure 2. Overview of experimental setup. Vehicles passed on right side, in same direction as cyclist.

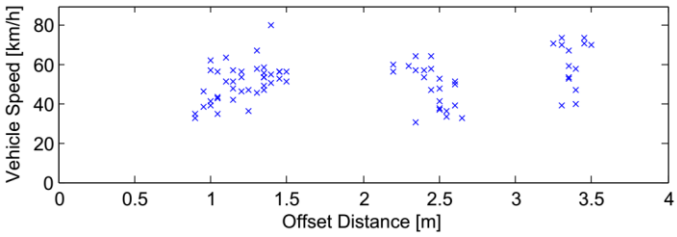

Figure 3. Test data speed and offset distances.

Measurements of lateral force, lateral wind speed component and static pressure from a typical run are shown in Figure 4. The data is presented time-offset based on the vehicle speed, so that the three traces represent measurements that would be observed at a single location for any given time.

Lorca et al. [2], and Lichtneger and Ruck [11] suggest that the lateral force F on a roadside object might be modeled as

$$C_f = 2F/\rho A_v U_v^2 \quad (1)$$

where ρ is air density, A_v is frontal area of the passing vehicle and U_v is the relative velocity of the passing vehicle. The coefficient C_f is a dimensionless value that accounts for the streamlining and shape of both the passing vehicle and the cyclist. A peak pressure difference coefficient C_p can be similarly defined as

$$C_p = 2P/\rho U_v^2 \quad (2)$$

where P is ρ is air density and U_v is the relative velocity of the passing vehicle. The coefficient C_p is a dimensionless force coefficient with a similar role to C_f.

The initial pulse of pressure and air velocity (and resulting transient moment on the cyclist) are larger than any of the fluctuations that followed, both in terms of overall magnitude, and in terms of time rate of change of the quantities. In this study, the magnitude of the difference between the first positive peak and negative "peaks" of pressure, air speed and moment were extracted from the time-series data for each run. (For example, in Fig. 4, the peak differences in pressure, force and wind speed are 20 Pa, 6.4 N and 2.0 m/s, all occurring within the first second.)

Fig. 5 shows the measured peak force difference versus measured peak pressure difference. (While the experiment was configured to measure a torque, all tests had the same moment arm and the load cell itself measures force.) The relationship between the two is approximately linear, within measurement uncertainty. This suggests measurements of pressure, which are simpler experimentally and can be found in the literature (e.g. Lichtneger and Ruck [11] or Sanz-Andrés and Santiago-Prowald [12]) can be used to give reasonable approximations of the side force (or moment) that could be expected on a cyclist.

Fig. 6 shows the peak differences of pressure, force and wind speed U as a function of offset distance. It can be argued that offset distance could be normalized by the square root of the vehicle frontal area, however, verification of this theory was not possible since only a single vehicle was tested.

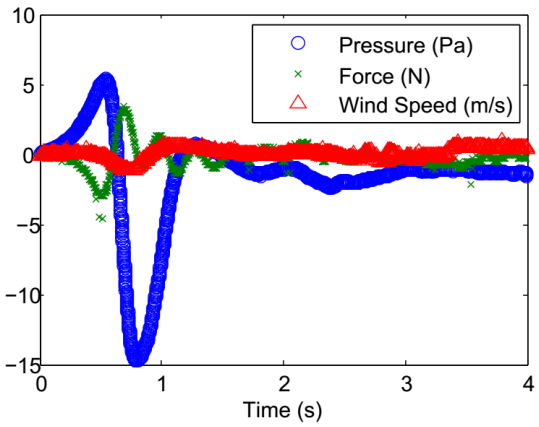

Figure 4. Example pressure, load cell force and wind speed magnitude. Vehicle speed 53.3 km/h, offset distance 1.35 m.

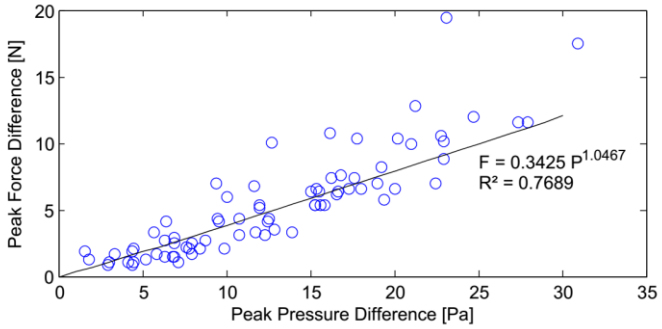

Figure 5. Peak differences in pressure and force observed for each test case.

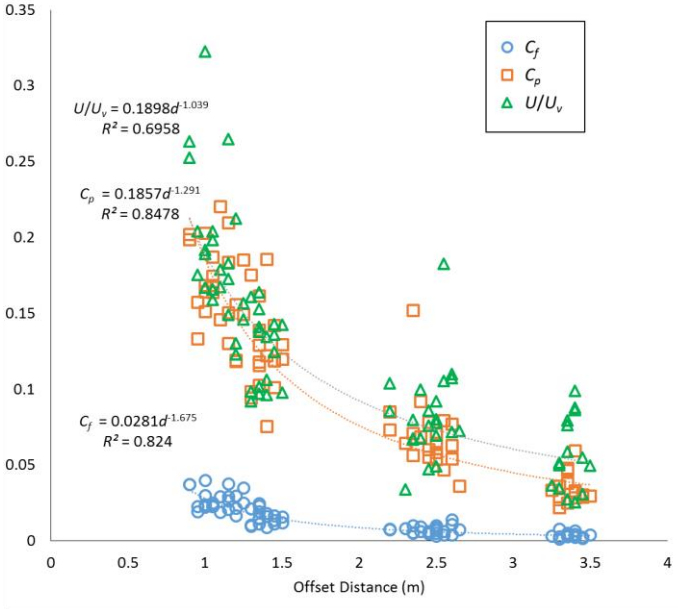

Figure 6. Measured peak differences versus offset distance.

Fig. 7 shows an updated version of Fig. 1 based on the experimental measurements presented here. Peak force was assumed to vary with vehicle velocity squared, and the measured force was used with Eqn. 2 and the fit equation for C_f in Fig. 6. The resulting forces were multiplied by 0.59 m (the experimental moment arm) to get tipping moments, in N·m. This gives a predictive equation for tipping moment M of

$$M = \frac{1}{2}\rho A_v U_v^2 (0.0281 d^{-1.675}) L \qquad (3)$$

where L is the experimental moment arm (0.59 m) and d is the offset distance in units of meters.

Although no supporting evidence was found for the 17 N "tolerance limit" reported (and re-reported in the literature) [3-6], here it has been converted to a moment by multiplying by the 0.87 m centroid height of the bike and rider in this experiment (Table 1) and is included in Fig. 7 for comparison purposes. Due to the power law relation used to fit the data, the model shown in Fig. 7 is unrealistic at offset distances less than about 1 m. Since offset distance is measured from vehicle side to the centerline of the cyclist, vehicles passing with offsets much less than 1 m would risk physically contacting the cyclist.

Both experimental results (Fig. 6) and the tipping moment model (Eqn. 3; Fig. 7) suggest that tipping moment decreases asymptotically with offset distance. No supporting evidence was found to support the assumption of no forcing at offset distances greater than 3.0 m shown in Fig. 1. The magnitudes of the experimental forces and moments, and those predicted by the resulting model, were of similar magnitude to those in Fig. 1 and those observed by Lichtneger and Ruck [11] for a small flat surface alongside a roadway at cyclist height.

Finally, readers are cautioned that the uncertainty of Fig. 7 is high, owing to the scatter in the experimental data from which it was derived and the limited nature of these preliminary experiments (e.g. only one test vehicle).

IV. Conclusions

The results of this experimental study suggest that the peak forcing on a bicycle is reasonably well correlated to the peak static pressure pulse (within experimental scatter), and also to the peak wind speed magnitude. This means that (1) measurements of wind speed and/or pressure may be sufficient in future experiments, and (2) extrapolation from studies of similar objects, such as signs and walls near roadways, should likely give representative forcing for bicycles.

The relationship in Fig. 1 appears to be a reasonably practical approximation for general planning. The most notable deficiency is that vehicle size and aerodynamic considerations are not illustrated. Fig. 7 presents a possible improvement to this relationship, however, it is not yet validated. During this study, it became apparent that there is little understanding of what levels and types of transient forcing cyclists can safely compensate for in practice. This would be an interesting and relevant area for future investigation.

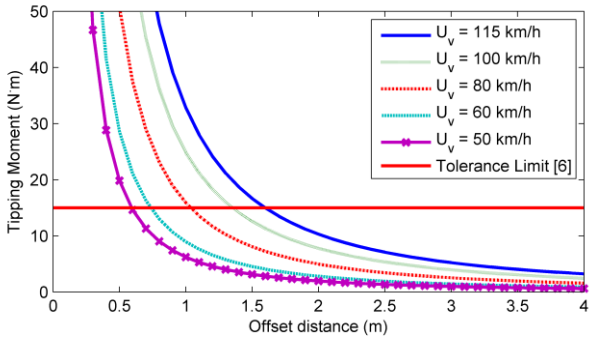

Figure 7. Estimated tipping moments for the cyclist and vehicle from the current study.

Acknowledgment

Mr. Rubie's work on this project was supported by a University of Guelph Undergraduate Research Assistant grant.

References

[1] Khan, A. M, Bacchus, A. Bicycle Use of Highway Shoulder. Transportation Research Record 1502. Nat. Academy Press. 8-21. 1995.

[2] Llorca, C., Angel-Domenech, A., Agustin-Gomez, F., Garcia, A. Motor vehicles overtaking cyclists on two-lane rural roads: analysis on speed and lateral clearance. Safety science. 92, 302-310. 2017.

[3] Hudson, M. Bicycle Planning. Architectural Press, London. ISBN 0-85139-058-7. 1982.

[4] MTO (Ministry of Transportation, Ontario). Ontario Bikeways Planning and Design Guidelines. ISBN 0-7778-5350-7. March, 1996.

[5] Vélo Québec. Technical Handbook of Bikeway Design. ISBN 2-9801944-4-1. 1992.

[6] Smith, D. T. Safety & Locational Criteria for Bicycle Facilities User Manual Vol. 1 Bicycle Facility Locational Criteria. Report FHWA-RD-75-113. U. S. Federal Highway Administration. Feb., 1976.

[7] Walton, D., Dravitzki, V. K., Cleland, B. S., Thomas, J. A., Jackett., R. Balancing the Needs of Cyclists and Motorists. Land Transport New Zealand Research Report 273. 2005.

[8] Cali, P. M., Covert, E. E. Experimental Measurements of the Loads Induced on an Overhead Highway Sign Structure by Vehicle-Induced Gusts. J. Wind Eng. & Ind. Aero. 84, 87-100. 2000.

[9] Quinn, A. D., Baker, C. J., Wright, N. G. Wind and Vehicle Induced Forces on Flat Plates – Part 2: Vehicle Induced Force. J. Wind Eng. & Ind. Aero. 89, 831-847. 2001.

[10] Sanz-Andrés, A., Laverón, A., Cuerva, A., Baker, C. Vehicle-Induced Force on Pedestrians. J. Wind Eng. & Ind. Aero. 92, 185-198. 2004.

[11] Lichtneger, P., Ruck, B. Full scale experiments on vehicle induced transient loads on roadside plates. J. Wind Eng. & Ind. Aero. 136, 73-81. 2015.

[12] Sanz-Andrés, A., Santiago-Prowald, J. Train-Induced Pressure on Pedestrians. J. Wind Eng. & Ind. Aero. 90, 1007-1015. 2002.

[13] Gerhardt, H. J., Krüger, O. Wind and Train Driven Air Movements in Train Stations. J. Wind Eng. & Ind. Aero. 74-76, 589-597. 1998.

[14] Moulton, A., Hadland, A., Milliken, D. Aerodynamic Research Using the Moulton Small-Wheeled Bicycle. Proc. IMechE Part A: J. Power and Energy. 220, 189-193. 2006.

[15] Tew, G. S., Sayers, A. T. Aerodynamics of Yawed Racing Cycle Wheels. J. Wind. Eng. & Ind. Aero. 82, 209-222. 1999.

[16] Robertson, P. A direction-insensitive static head sensor. Journal of Physics E (Scientific Instruments), v 5, n 11, p 1080-2. 1972.

[17] Kyle, C. R. Reduction of Wind Resistance and Power Output of Racing Cyclists and Runners Travelling in Groups. Ergonomics. 22 (4), 387-397. 1979.

[18] Eowsakul, V., Ortolani, T. Improving the aerodynamic characteristics of a Dodge Ram pickup truck. ASME IMECE Paper No. 97-WA/DE-18, 8p, 1997.